High thermoelectric performance of bornite through control of the Cu(II) content and vacancy concentration

Article

Accepted Version

Article

High thermoelectric performance of bornite through control of the Cu(II) content and vacancy concentration

Sebastian O. J. Long, Anthony V. Powell, Paz Vaqueiro, and Stephen Hull

Chem. Mater., **Just Accepted Manuscript** • DOI: 10.1021/acs.chemmater.7b04436 • Publication Date (Web): 13 Dec 2017

High thermoelectric performance of bornite through control of the Cu(II) content and vacancy concentration

Sebastian O. J. Long,[a] Anthony V. Powell*,[a] Paz Vaqueiro,[a] Stephen Hull[b]

a. Department of Chemistry, University of Reading, Whiteknights, Reading, RG6 6AD, UK.

b. ISIS Facility, Rutherford Appleton Laboratory, Harwell, Oxford, Didcot, OX11 0OX, UK

.

The thermoelectric performance of the p-type semiconductor bornite, Cu_5FeS_4, is greatly enhanced through chemical substitution. Non-stoichiometric materials in which the Cu:Fe ratio and overall cation-vacancy content were adjusted are reported and a figure of merit, ZT = 0.79, is achieved at temperatures as low as 550 K in $Cu_{4.972}Fe_{0.968}S_4$. All materials were synthesised mechanochemically and characterised by powder X-ray diffraction, DSC and thermal and electrical transport property measurements. Single-phase behaviour is retained in copper deficient phases, $Cu_{5-x}FeS_4$, for vacancy levels up to x = 0.1, while in materials $Cu_{5+y}Fe_{1-y}S_4$, in which the Cu:Fe ratio is varied whilst maintaining full occupancy of cation sites, single-phase behaviour persists for y≤0.08. Adjusting the Cu:Fe ratio at a constant cation-vacancy level of 0.06 in $Cu_{4.94+z}Fe_{1-z}S_4$, leads to single-phases for z ≤0.04. DSC measurements indicate the temperature of the intermediate- (2a) to high-temperature (a) phase transition shows a more marked dependence on the Cu:Fe ratio than the lower temperature 4a to 2a transition. The thermoelectric power factor increases almost linearly with increasing Cu(II) content. The maximum figures of merit are obtained for materials with Cu(II) contents in the range 0.10 to 0.15 (corresponding to 2.0 – 2.8 % Cu(II)) which simultaneously contain ca. 1 % of cation vacancies.

Introduction

Thermoelectric (TE) materials have the potential to generate electrical energy from otherwise waste heat.[1] This offers opportunities to achieve more efficient use of precious fossil fuel resources[2] and also to enhance the energy recovery from renewable sources such as photovoltaic devices.[3,4] Of the range of sources of waste heat available, that produced in industrial processes offers particularly attractive prospects for large-scale implementation of TE technology. Over 80% of the waste heat generated in industrial processes is at temperatures in the range 373 ≤ T/K ≤ 575,[5,6] suggesting considerable opportunities exist for the development of efficient TE materials that operate in this region.

Current commercial thermoelectric devices are based on bismuth telluride.[7,8] The combination of the low abundance of tellurium coupled with comparatively low TE efficiencies has restricted wide-scale adoption of TE technology. This has led to a major world-wide research effort to develop new materials for thermoelectric energy conversion. Whilst significant advances have been achieved in the figure of merit ($ZT = S^2\sigma T/\kappa$) at high temperatures, there remains a dearth of materials suitable for energy recovery from waste heat in the low to mid-range of temperatures appropriate to industrial processes.

Much of the recent research effort has focused on chalcogenides and there has been a growing realisation that mineral-type phases offer considerable potential as earth-abundant thermoelectrics.[9–15] For example, tetrahedrites have been shown to be promising p-type materials, reaching maximum figures of merit, ZT > 1, at elevated temperatures.[16,17] Similarly, work by Snyder *et. al.*[18] has shown that a non-stoichiometric cuprous sulphide, $Cu_{2-x}S$, exhibits an exceptionally low thermal conductivity, which results in a figure-of-merit, ZT = 1.7 at 1000 K. It has been suggested that this remarkably low value for a crystalline phase arises from the copper sub-lattice entering a liquid-like state on heating, due to the high-mobility of the copper cations.[19] The combination of a liquid-like thermal conductivity with electrical transport properties determined by the crystalline sulphide sub-lattice has led this class of material to be termed Phonon-Liquid Electron-Crystals (PLECs).[19,20] However, despite the high performance, the copper-ion mobility in $Cu_{2-x}S$ leads to degradation of the material through ion migration under constant current.[21,22] Therefore there is growing interest in discovering alternative materials with PLEC characteristics, in which ion migration can be suppressed.

Bornite, Cu_5FeS_4, is an abundant copper-iron sulphide mineral which at high temperatures adopts a cation-deficient anti-fluorite structure similar to that of $Cu_{2-x}S$. Stoichiometric bornite possesses a similarly low thermal

conductivity to $Cu_{2-x}S$. However, the presence of iron on the cation sites helps suppress copper ion migration, with no significant degradation in electronic properties occurring when a test sample is maintained under constant current.[23] Bornite-related phases are therefore promising candidates for TE applications, providing the low power factor ($S^2\sigma$) of stoichiometric bornite can be improved.

Above 530 K, bornite adopts an anti-fluorite type structure (Fig. 1) in which the cubic unit cell (space group: $Fm\bar{3}m$) contains two cation vacancies.[24,25] These, together with the copper and iron cations, are distributed over the eight available cation sites in a statistical fashion. On cooling below 540 K, ordering of vacancies results in a supercell with lattice parameters related to those of the cubic high-temperature phase (a_p) by $2a_p \times 2a_p \times 2a_p$ (Fig. 1b), termed the 2a structure. Further cooling below 460 K, leads to an orthorhombic (space group $Pbca$)[26] $4a_p \times 2a_p \times 2a_p$ unit cell, denoted 4a, in which zinc blende and anti-fluorite sub-cells alternate. Although the distribution of copper and iron cations in the 4a and 2a structures has not been established unambiguously, ordering schemes have been suggested by Ding *et. al.*[27]

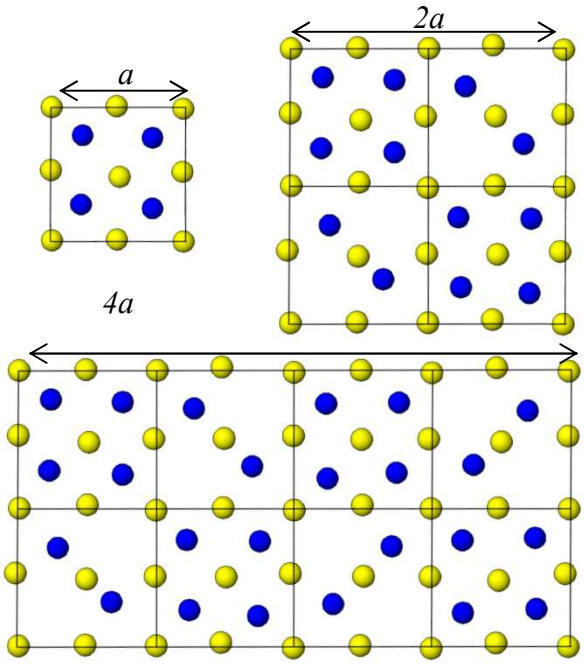

Figure 1. View of the vacancy ordering in the three phases of Cu5FeS4: (a) high-temperature phase (2a) intermediate-temperature phase (4a) low-temperature phase. Key: Cu/Fe, blue circles; S, yellow circles. Zinc-blende and anti-fluorite unit cells are outlined.

Here, we describe how the electron-transport properties of bornite may be markedly improved through judicious control of composition and cation-vacancy levels. We demonstrate that significant enhancements in the power factor ($S^2\sigma$) may be achieved without impacting on the thermal conductivity (κ). This leads to an increase of up to 88% in the figure of merit, with a maximum value of ZT = 0.79 being attained in $Cu_{4.972}Fe_{0.968}S_4$ at the remarkably low temperature of 550 K: a temperature directly relevant to low-grade waste heat.

Experimental Procedure and Synthesis

2.1 Starting material and synthesis. All samples were prepared from mixtures of copper, (99.5%, Sigma Aldrich) iron (99.9+%, Sigma Aldrich) and sulphur (flakes, 99.99%, Sigma Aldrich) of the appropriate stoichiometry. After grinding mixtures of the powdered elements together in an agate mortar, the mixture was placed in a 25 mL stainless-steel jar under an argon atmosphere and 6mm stainless-steel balls added (2:5 mass ratio of powder to balls). Two successive millings, each of 20 h, were carried out using a Retsch PM100 Planetary Ball Mill operating at 500 rpm with a change of rotational direction every 5 mins, The resulting powder was loaded into a tungsten carbide mould, sandwiched between graphite foils and tungsten carbide plungers. The mould was heated to 823 K, under a nitrogen atmosphere, and a pressure of 90 MPa applied for 30 minutes in order to consolidate the powder.

Three series of materials were prepared: $Cu_{5-x}FeS_4$ ($-0.08 \le x \le 0.16$) allowed exploration of the impact of varying copper content at a fixed iron content, whilst $Cu_{5+y}Fe_{1-y}S_4$ ($0.02 \le y\ 0.10$) and $Cu_{4.94+z}Fe_{1-z}S_4$ ($0.02 \le z \le 0.10$) enabled investigation of the effect of the substitution of copper for iron at a constant overall cation content, corresponding to a fully occupied or cation-deficient cation sub-lattice respectively.

2.3 Sample Characterization. Consolidated samples were polished by hand, producing cylindrical pellets with a diameter ca. 12.66mm (±0.03 mm) and thickness between 1-2mm (±0.03 mm). Densities were measured on an Archimedes ADAM PW184 balance. Sample densities were close (> 98%) to the crystallographic density of stoichiometric bornite. Powder X-Ray diffraction data were collected using a Bruker D8 Advance (Cu-$K_{\alpha 1}$: λ = 1.5405Å) diffractometer fitted with a LynxEye linear detector and a Ge monochromator. All Le Bail refinements using powder X-ray diffraction data were carried out using the GSAS software package.[28]

Elemental compositions were determined using EDX on a FEI Quanta FEG 600 Environmental Scanning Electron Microscope (ESEM) under a high-vacuum, using a maximum voltage of 20 kV on pelletized samples. An Oxford Instruments EDX spectrometer was used, calibrated using a standard block supplied by Micro-Analysis Consultants Ltd. DSC measurements were carried out on a TA DSC2000 instrument on powdered samples loaded into aluminium pans. Data were collected on both heating and cooling with heating and cooling rates of 10 K min^{-1} and 20 K min^{-1} respectively. The 4a→2a (T1) transition temperature was determined from the peak maximum whilst the 2a→a (T2) transition temperature was determined from the change in gradient, owing to the glass-like nature of the DSC transition.

2.4 Transport Properties. Thermoelectric property data were collected over the temperature range 300 ≤ T/K

≤ 580. The upper limit for the collection of physical property data was selected following the observation by Guelou *et al.* that stoichiometric bornite (Cu_5FeS_4) begins to lose sulphur above 600 K under a flowing nitrogen atmosphere.[29] The electrical resistivity, (ρ), and Seebeck coefficient, (S), were measured simultaneously under a slight over pressure of He using a Linseis LSR-3 instrument. A gradient of 50 K was maintained across the sample for the measurement of the Seebeck coefficient. The resistivity was measured using a 4-probe DC method, with the two central thermocouple probes (8 mm separation) aligned perpendicular to the terminal Pt electrodes.

The thermal diffusivity of graphite coated pellets was measured using a Netzsch LFA 447 NanoFlash system over the temperature range 300 ≤ T/K ≤ 580. Higher temperature measurements (573 ≤ T/K ≤ 700 K) were performed using an Anter Flashline 3000 instrument. Data were analysed using Cowan's model with a pulse correction applied.[30] The thermal conductivity was determined using the calculated Dulong-Petit heat capacity for Cu_5FeS_4 (Cp=0.497 J K^{-1} g^{-1}).

Results and Discussion

3.1 Structural Characterisation and Phase Behaviour. Powder X-Ray diffraction data for the product of hot pressing a ball-milled mixture of composition Cu_5FeS_4 are indexable on the basis of an orthorhombic unit cell, a=10.953(1) Å, b=21.8694(16) Å, c=10.9464(10) Å, consistent with the formation of a single phase of the low-temperature (4a) phase of stoichiometric bornite. Whilst HRTEM studies by Ding *et. al.* suggest that domains of 1a, 2a, 4a and 6a may exist at room temperature,[31] analysis of the powder X-ray diffraction data presented here (Fig. 2) provide no evidence for the presence of domains of this type.

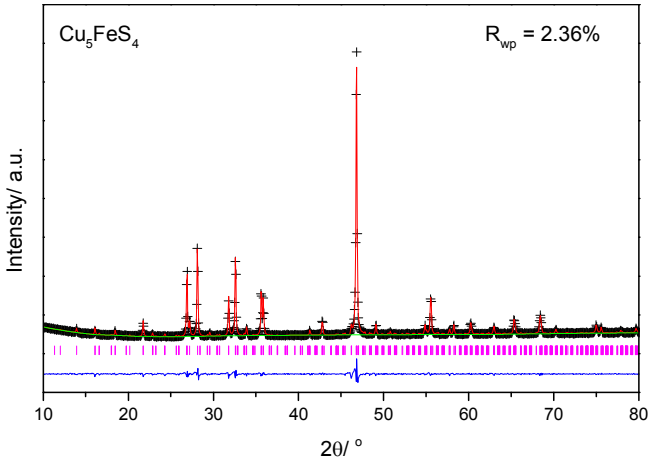

Figure 2. Powder X-ray diffraction data for Cu_5FeS_4, together with analysis by the structure-independent Le Bail method, where the observed, calculated and difference profiles are denoted by crosses, the red solid line and the lower full line respectively. Markers represent the reflection positions for the low-temperature phase of Cu_5FeS_4 (space group *Pbca*).

Powder X-ray diffraction data for materials in the series $Cu_{5-x}FeS_4$ (-0.08 ≤ x ≤0.16) show the presence of a bornite-related phase, indexable on an analogous unit cell to that for the stoichiometric phase, at all compositions. Reflections arising from a chalcopyrite ($CuFeS_2$) impurity are evident at x ≥ 0.10 (Fig. 3a). Within the detection limits of powder X-ray diffraction, samples with x < 0.10 are single phase. The lattice parameters of the bornite-type phase (Supplementary Information) are relatively insensitive to the total copper content; variations of < 1% being observed in the orthorhombic lattice parameters across the entire range of compositions investigated.

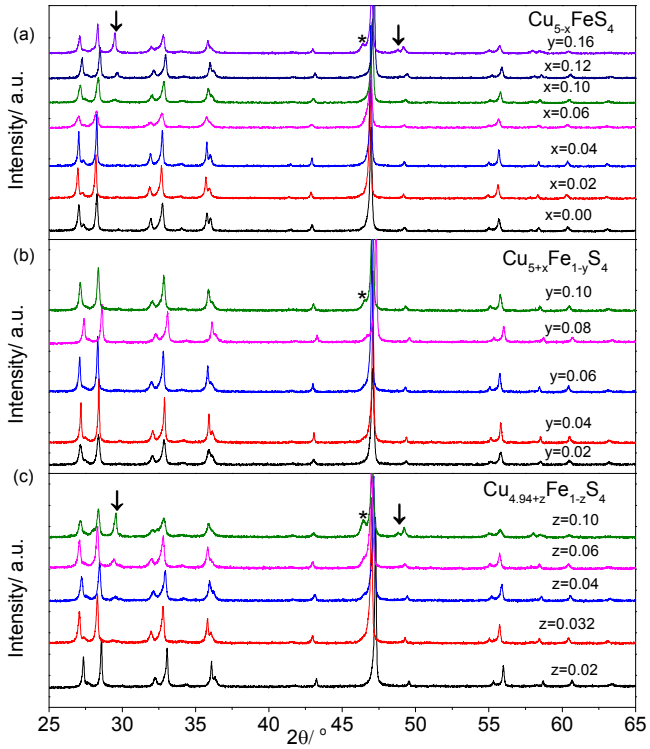

Figure 3. Powder X-Ray Diffraction patterns for selected bornite samples in the series (a) $Cu_{5-x}FeS_4$, (b) $Cu_{5+y}Fe_{1-y}S_4$ and (c) $Cu_{4.94+z}Fe_{1-z}S_4$, over the angular range 25 ≤ θ/° ≤ 65. Peaks corresponding to a $CuFeS_2$ impurity have been marked with an arrow, and those corresponding to $Cu_{1.8}S$ with an asterix.

Powder X-ray diffraction data (Fig. 3b) for materials in the series $Cu_{5+y}Fe_{1-y}S_4$ reveal single phase behaviour up to y = 0.08. At higher values of y, there is evidence for the formation of trace amounts of a digenite ($Cu_{1.8}S$) impurity. Lattice parameters (Supplementary Information) show a similarly low sensitivity to composition as the copper deficient phases described above, with < 1% variation being observed in each of the orthorhombic unit-cell parameters across the series.

The investigation of the impact of the substitution of copper for iron in cation-deficient phases ($Cu_{4.94+z}Fe_{1-z}S_4$) establishes an upper limit of z ≤ 0.04 for single-phase behaviour. Powder X-ray diffraction data (Fig. 3c) reveal that at increasing levels of copper substitution, a chalcopyrite impurity is formed, with digenite appearing at the highest level of non-stoichiometry (z = 0.1). The orthorhombic lattice parameters of the bornite-type phase (Supplementary Information) again show <1% variation

across the range of composition. Contrary to the behaviour of fully-stoichiometric bornite-type phases ($Cu_{5+y}Fe_{1-y}S_4$), where impurities appear at Cu:Fe ratios above 5.52, in cation-deficient phases chalcopyrite formation occurs above a lower Cu:Fe threshold of 5.19:1. This suggests there is a complex dependence of the phase behaviour on the composition and defect concentration in this region of the copper-iron-sulphur phase diagram.

Table 1. Elemental compositions for selected samples determined by EDX analysis.

Nominal	Experimental
Cu_5FeS_4	$Cu_{5.00(2)}Fe_{0.99(1)}S_4$
$Cu_{4.94}FeS_4$	$Cu_{4.91(2)}Fe_{1.00(1)}S_4$
$Cu_{4.9}FeS_4$	$Cu_{4.85(2)}Fe_{1.05(1)}S_4$
$Cu_{5.06}FeS_4$	$Cu_{5.14(1)}Fe_{0.91(1)}S_4$
$Cu_{5.08}Fe_{0.92}S_4$	$Cu_{5.06(2)}Fe_{0.94(1)}S_4$
$Cu_{4.972}Fe_{0.968}S_4$	$Cu_{4.89(2)}Fe_{1.02(1)}S_4$

The iron and copper contents of selected pelletized samples, determined experimentally by Analytical Electron Microscopy (EDX), are in reasonable agreement with the nominal compositions (Table 1).

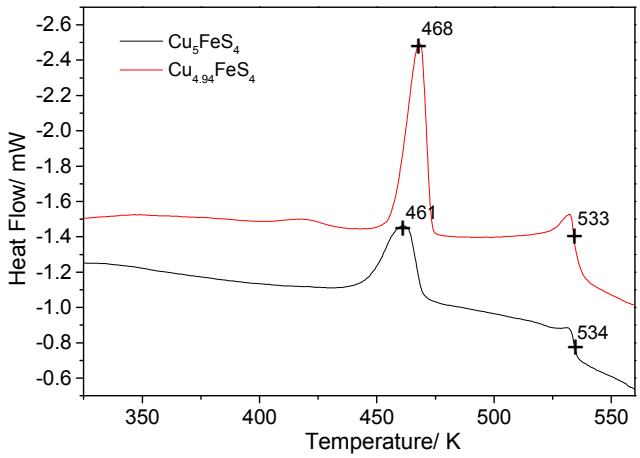

Figure 4. DSC data collected on heating for two bornite samples. Transition temperatures are shown.

DSC data collected on Cu_5FeS_4 on heating (Fig. 4) show two transitions at ca. 470 and 530 K, with a degree of hysteresis. These features can be assigned to the T1 (4a → 2a) and T2 (2a → a) phase transitions respectively. DSC data (Supplementary information) for materials of general formula $Cu_{5-x}FeS_4$ reveal that the introduction of cation vacancies has little effect on the T2 transition for compositions in the range $-0.08 \le x \le 0.1$, whilst the temperature of the lower temperature T1 transition decreases slightly with increasing x for $x \ge 0.02$. In the $Cu_{5+y}Fe_{1-y}S_4$ series, DSC data (Supplementary Information) show that the T2 transition temperature decreases from 534 K when y = 0 to 515 K when y = 0.1 , indicating that, at a constant vacancy concentration, the T2 phase transition is sensitive to the Cu:Fe ratio. The T1 transition temperature shows a markedly weaker dependence on the Cu:Fe ratio. The behaviour of the $Cu_{4.94+z}Fe_{1-z}S_4$ series (Supplementary Information) is similar to that of $Cu_{5+y}Fe_{1-y}S_4$, with the T2 phase transition temperature showing a marked dependence on the Cu:Fe ratio. The presence of impurities of $Cu_{1.8}S$ in the more highly-substituted copper-iron sulphides, results in an additional transition at ca. 370 K (Supplementary Information) corresponding to the low-to-high temperature phase transition of digenite.[32,33] These results are broadly consistent with a previous DSC study on a range of natural and synthetic samples of bornite, which concluded that the temperature of the T2 phase transition is linearly dependent on the Cu:Fe ratio and the Fe content, whilst no correlation is observed between the T1 phase transition temperature and the composition.[33]

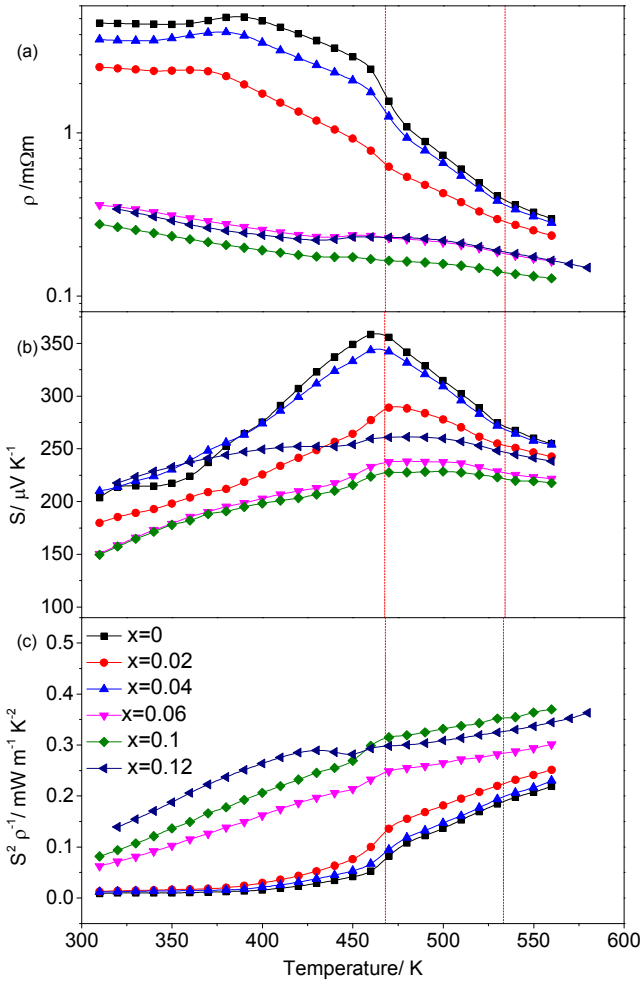

Figure 5. Temperature dependence of the electrical transport properties of $Cu_{5-x}FeS_4$ ($0 \le x \le 0.12$): (a) electrical resistivity; (b) Seebeck coefficient; (c) power factor. Red vertical lines indicate the temperatures of the T1 and T2 structural phase transitions in Cu_5FeS_4.

3.2 Thermoelectric Properties. The physical properties of the stoichiometric parent compound, Cu_5FeS_4, are in excellent agreement with those from previous work on the TE properties of bornite [23,29,34,35] and provide a benchmark for the investigation of the non-stoichiometric materials. The Seebeck coefficient of Cu_5FeS_4 exhibits a maximum of ca. 350 μV K^{-1} at 460 K (Fig. 5), and remains positive over the entire temperature range investigated, indicating that holes are the dominant charge carriers throughout. The temperature dependence of the electrical

resistivity is consistent with semiconducting behaviour and shows an anomaly at the temperature of the T1 phase transition, coinciding with the maximum in the Seebeck coefficient. By contrast, there is little signature of the higher temperature T2 phase transition in the electrical property data. However, the T2 phase transition is reflected in the minimum in the thermal conductivity (ca. 0.3 W m^{-1} K^{-1}) of Cu_5FeS_4 (Fig. 6) at 550 K. The maximum value of the figure of merit for stoichiometric bornite, ZT = 0.44 at 550K, is in good agreement with previous reports of the figure of merit at 550 K, which indicate values in the range 0.3 ≤ ZT ≤ 0.55.[23,29,34,35]

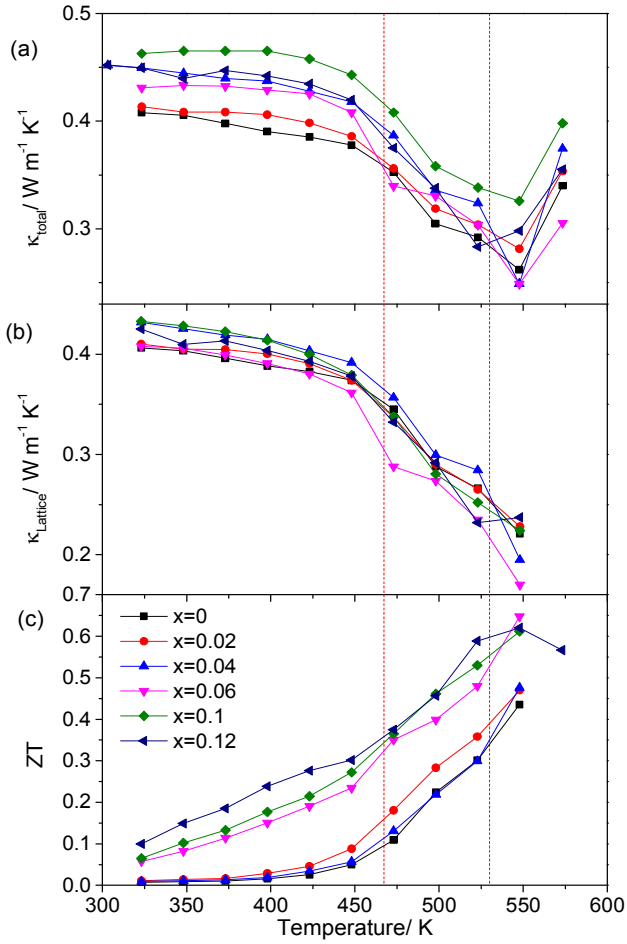

Figure 6. Temperature dependence of: (a) thermal conductivity; (b) lattice thermal conductivity; (c) thermoelectric figure of merit for $Cu_{5-x}FeS_4$ (0 ≤ x ≤ 0.12). Red vertical lines indicate the temperatures of the T1 and T2 structural phase transitions in Cu_5FeS_4.

Electrical measurements for $Cu_{5-x}FeS_4$ materials with both increased (x < 0) and decreased (x > 0) copper contents were attempted. However, materials in the former category exhibit relatively high electrical resistivities (e.g. ρ = 86 mΩ m at 300 K for x= -0.06), preventing full thermoelectric characterisation. Therefore compositions in the range -0.8 < x < 0.0 will not be discussed further. For copper deficient materials, $Cu_{5-x}FeS_4$, (0.0 < x ≤ 0.12) (Fig. 5), ρ(T) is consistent with semiconducting behaviour throughout the compositional range. With increasing levels of copper deficiency the resistivity and the Seebeck coefficient decrease. Given the formulation $Cu^{I}_5Fe^{III}S_4$ of the end-member phase proposed by Townsend *et. al.*,[36] on the basis of Mössbauer spectroscopic and magnetic data, reducing the copper content would be expected to result in an increase in the concentration of holes, which would account for the observed reduction in electrical resistivity. The anomaly in both ρ(T) and S(T) in the region of the T2 transition is less marked for compositions in the middle of the range investigated.

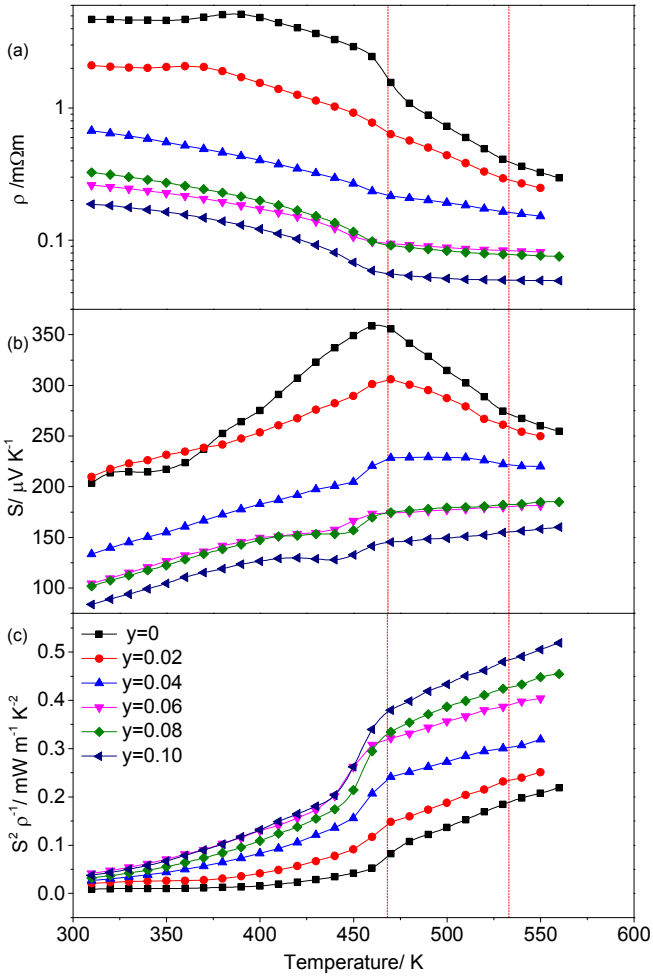

Figure 7. Temperature dependence of the electrical transport properties of $Cu_{5+y}Fe_{1-y}S_4$ (0≤y≤0.1): (a) electrical resistivity; (b) Seebeck coefficient; (c) power factor. Red vertical lines indicate the temperatures of the T1 and T2 structural phase transitions in Cu_5FeS_4.

All materials of general formula, $Cu_{5-x}FeS_4$, exhibit a low thermal conductivity for compositions with x ≤ 0.12: values at room temperature lying the in the range 0.4 - 0.5 W m^{-1} K^{-1} (Fig. 6). Materials with x < 0.12 exhibit a minimum in κ(T) at temperatures (ca. 550 K) in the region of the T2 phase transition. Whilst the thermal conductivity for materials in this compositional range shows little dependence on copper content, the lattice contribution to the thermal conductivity (κ_L), determined by subtraction of the electronic component calculated using the

Wiedemann-Franz law ($L = 2.44 \times 10^{-8}$ W Ω K^{-2}), suggests that copper deficiency increases κ_L slightly from that of the stoichiometric parent compound (Fig. 6). All samples in this series exhibit an increase in thermoelectric performance when compared to the parent bornite phase,[23,29] with considerable enhancements in the figure of merit: $0.61 < (ZT)_{max} < 0.65$ (Fig. 6), being achieved for compositions with $0.06 \leq x \leq 0.12$.

Resistivity data for materials of general formula $Cu_{5+y}Fe_{1-y}S_4$ are consistent with semiconducting behaviour (Fig. 7). The resistivity shows substantial reductions with increasing copper content, as the hole concentration increases. There is a concomitant reduction in Seebeck coefficient, which remains positive at all compositions and temperatures. The decrease in resistivity outweighs the reduction in Seebeck coefficient and as result the TE power factor increases with increasing copper content, exceeding 0.4 mW m^{-1} K^{-2} at $x > 0.04$ (Fig. 7).

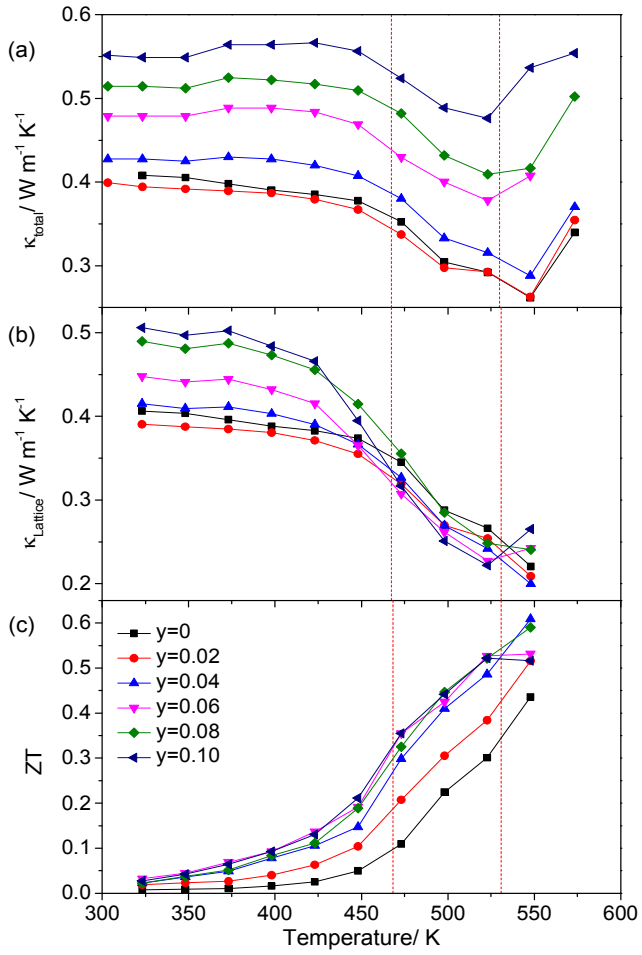

Figure 8. Temperature dependence of: (a) thermal conductivity; (b) lattice thermal conductivity; (c) thermoelectric figure of merit for $Cu_{5+y}Fe_{1-y}S_4$ ($0 \leq y \leq 0.1$). Red vertical lines indicate the temperatures of the T1 and T2 structural phase transitions in Cu_5FeS_4.

All materials in the $Cu_{5+y}Fe_{1-y}S_4$ series exhibit a thermal conductivity below 0.6 W m^{-1} K^{-1} (Fig. 8): the value increasing with increasing copper content. This is due to the increased charge-carrier contribution, κ_e, evidenced by the reduction in electrical resistivity. There is a minimum in κ(T) in the region of the T2 phase transition. The reduction in the temperature at which this minimum occurs with increasing copper content, is consistent with the change in the temperature of the T2 transition determined using DSC. The decreasing thermal conductivity, as the T2 phase transition is approached, coupled with the increase in power factor, results in a significant enhancement in the figure of merit for materials over the entire range of compositions studied and maximum values exceed ZT = 0.59 at compositions corresponding to x=0.04 and 0.08. This is consistent with the observations of Qiu *et. al.*[23] who report that slight deviations from a 5:1 Cu:Fe ratio results in improvements in thermoelectric performance.

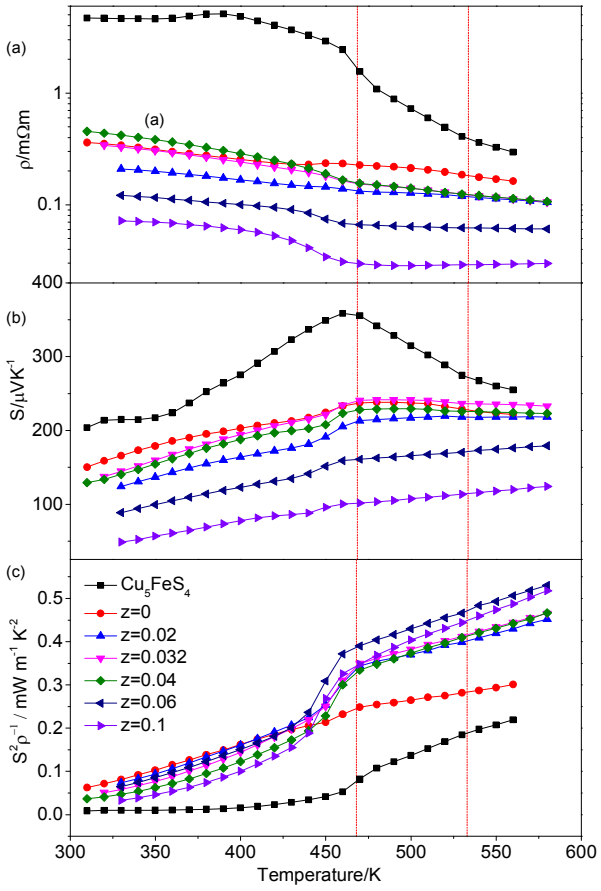

Figure 9. Temperature dependence of the electrical transport properties for $Cu_{4.94+z}Fe_{1-z}S_4$ ($0 \leq z \leq 0.1$): (a) electrical resistivity; (b) Seebeck coefficient; (c) power factor. Red vertical lines indicate the temperatures of the T1 and T2 structural phase transitions in Cu_5FeS_4. Data for Cu_5FeS_4 have been included for comparison purposes.

The substitution of copper for iron concomitantly with the introduction of cation vacancies in materials of general formula $Cu_{4.94+z}Fe_{1-z}S_4$ ($0.02 \leq z \leq 0.10$), produces further improvements in TE performance. p-type semiconducting behavior is retained at all compositions (Fig. 9) and both resistivity and Seebeck coefficient decrease with increasing copper content, analogous to the behavior observed in $Cu_{5-x}FeS_4$ and $Cu_{5+y}Fe_{1-y}S_4$. In $Cu_{4.94+z}Fe_{1-z}S_4$ there

is a compositional range over which the balance between improved electrical conductivity and reduced Seebeck coefficient is optimised and the power factor maximised (Fig. 9). In this region, there are significant enhancements in the power factor when compared to the cation-deficient (z = 0) parent phase, $Cu_{4.94}FeS_4$: the power factor at 550 K increasing from 0.29 mW m^{-1} K^{-2} at z = 0 to 0.42 mW m^{-1} K^{-2} at z= 0.04.

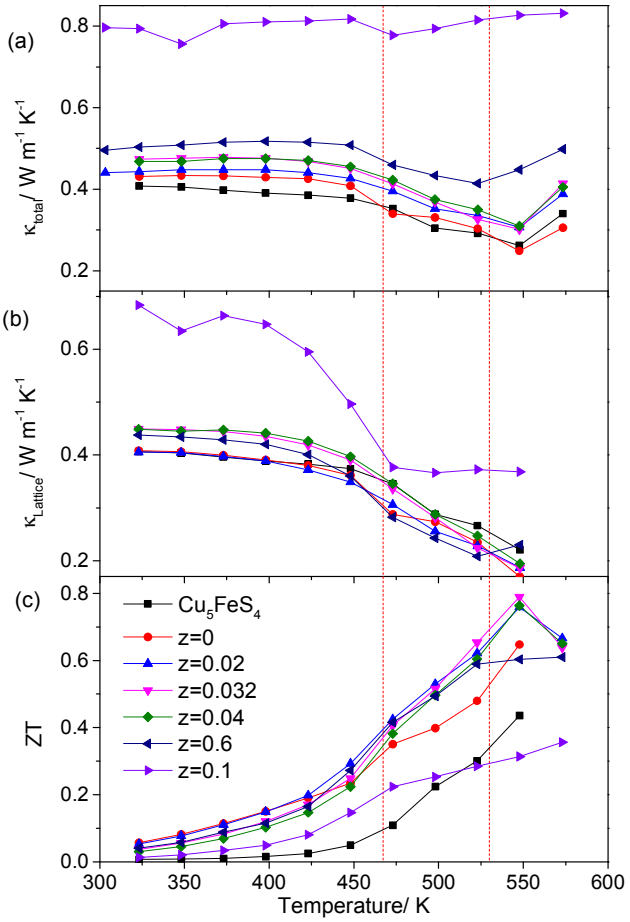

Figure 10. Temperature dependence of: (a) thermal conductivity; (b) lattice thermal conductivity; (c) thermoelectric figure of merit for $Cu_{4.94+z}Fe_{1-z}S_4$ (0 ≤ z ≤ 0.1). Data for Cu_5FeS_4 have been included for comparison purposes. Red vertical lines indicate the temperatures of the T1 and T2 structural phase transitions in Cu_5FeS_4.

With the exception of $Cu_{5.04}Fe_{0.9}S_4$, the thermal conductivity of all $Cu_{4.94+z}Fe_{1-z}S_4$ phases remains below 0.5 W m^{-1} K^{-1}, increasing only slightly with increasing copper content (Fig. 10). The significantly higher (ca. 0.8 W m^{-1} K^{-1}) thermal conductivity of $Cu_{5.04}Fe_{0.9}S_4$ is attributed to the presence of appreciable amounts of a chalcopyrite impurity, for which the thermal conductivity is in excess of 6 W m^{-1} K^{-1}. Although chalcopyrite has a reasonably high power factor at relatively low temperatures,[13] we have found that samples with high levels of chalcopyrite impurities have significantly higher thermal conductivities, and hence the best thermoelectric performances are always found for samples within the single-phase regions, as determined by powder X-ray diffraction.

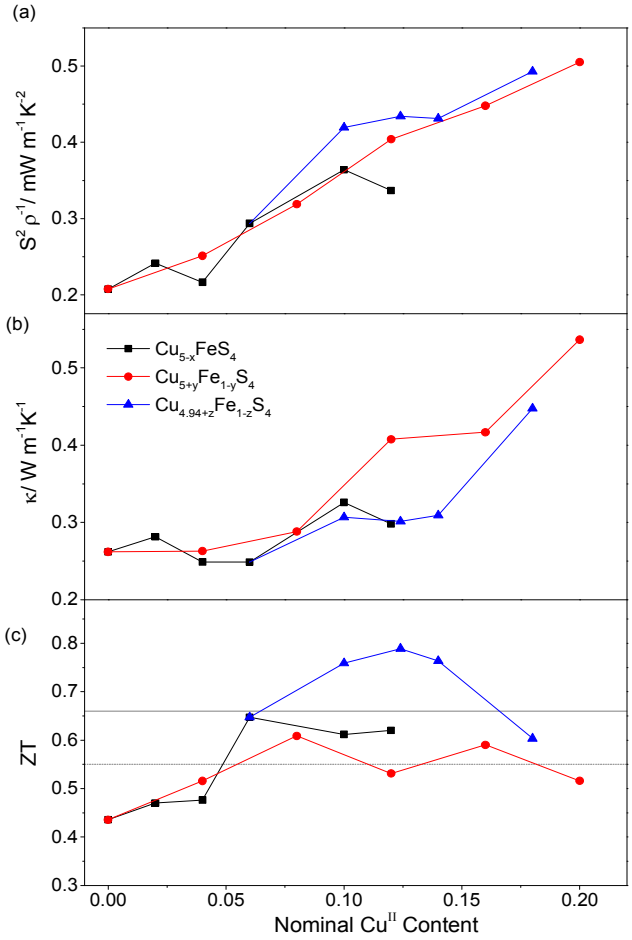

Figure 11. Thermoelectric properties of $Cu_{5-x+y}Fe_{1-y}S_4$ at 550K as a function of nominal Cu(II) content for single phase samples:(a) power factor; (b) thermal conductivity; (c) figure of merit. The solid grey line and the dashed grey line indicate the highest maximum ZT and highest ZT at 550K of thermoelectric bornites that have been reported (Table 2).

In the series $Cu_{4.94+z}Fe_{1-z}S_4$, the minimum in κ(T) shows no significant compositional dependence at compositions with z ≤ 0.04, but shifts to lower temperature for z > 0.04. This is analogous to the behaviour of $Cu_{5+y}Fe_{1-y}S_4$, in which the minimum in κ(T) also moved to lower temperatures above a critical Cu:Fe ratio corresponding to y = 0.04 (Fig. 8) and is consistent with the phase transition temperatures determined by DSC. The persistence of a negative dκ/dT to higher temperatures, where the power factor continues to increase, results in the highest figures of merit determined for bornite-related phases. The figure of merit of $Cu_{4.94+z}Fe_{1-z}S_4$ exceeds ZT = 0.76 for samples in the range 0.02≤ z ≤ 0.04, with the highest value of ZT = 0.79 being realised for $Cu_{4.972}Fe_{0.968}S_4$ (Fig. 10). This represents an 88% increase over the stoichiometric parent phase, Cu_5FeS_4. Moreover this performance is achieved at the remarkably low temperature of 550 K, suggesting that these materials are attractive candidates for energy recovery from low-grade waste-heat. The upper temperature for electrical and thermal transport property measurements was limited to 600 K owing to concerns over sample stability, including the reported appearance of a chalcopyrite-type phase above 550 K.[34] However, in previous

studies[23,29,34,35] of bornite-related phases, figures of merit at higher temperatures have been reported (Table 2) and the maximum value is generally achieved at ca. 700 K. Therefore the collection of thermal and electrical transport property data was extended to 700 K for a bornite-type phase close to the optimal composition, $Cu_{4.97}Fe_{0.93}S_4$, identified here (Supplementary Information). Between 550 and 700 K, both the power factor and the thermal conductivity increase with temperature leading to a slight further improvement, of approximately 8%, in the figure of merit achieving a value of ZT=0.84.

3.3 Stability and Application. A key consideration in the application of these materials is long-term stability, given the reported instability in materials such as $Cu_{2-x}S$ which exhibit PLEC behaviour, arising from the migration of copper ions under operating conditions.[22] It has been proposed that partial substitution of immobile cations into copper sites may be an effective means of suppressing the degradation of copper-containing PLEC materials.[37] This is supported by recent work on improving the stability of Cu_2Se by indium substitution.[38] In order to assess the success of this strategy in the high-performance bornite phase, $Cu_{4.972}Fe_{0.968}S_4$, measurements of electron transport properties on heating were carried out repeatedly over the temperature range $300 \leq T/K \leq 575$ (Supplementary Information). No significant change in the TE power factor was observed over the course of eight measurements. This suggests that the presence of the immobile iron cation at tetrahedral sites in the materials reported may indeed suppress diffusion of copper ions by effectively blocking the diffusion pathway.

Previous magnetic and spectroscopic studies of the parent Cu_5FeS_4 phase are consistent with Cu(I) and Fe(III) formal oxidation states,[36,39,40] and the introduction of holes requires the oxidation of one of the transition-metal elements. Whilst the presence of Fe(IV) in a sulphide environment would be highly unlikely, a number of mixed valent copper sulphides, containing Cu(I) and Cu(II) are known, including $Cu_{12}Sb_4S_{13}$[41] and $Cu_{22}Fe_8Ge_4S_{32}$,[42] Therefore, the three series of bornite-related phases reported here may be directly compared by consideration of the hole content arising from the formation of Cu(II) as a result of chemical substitution (Fig. 11). All materials may be formulated as $Cu_{5-x+y}Fe_{1-y}S_4$, with the nominal Cu(I) and Cu(II) contents given by (5-2x-y) and (x+2y) respectively. This illustrates that the substitution of iron by copper has a greater impact on the nominal Cu(II) content than does copper deficiency and therefore a larger hole concentration(Cu(II) content) may be achieved with smaller deviations from the stoichiometric composition. The power factor for all three series fall on a common trend line and increases almost linearly with Cu(II) content up to the maximum level of 0.2 Cu(II) achievable through chemical manipulation.

The thermal conductivity shows a more complex dependence on Cu(II) content. Phases in which full occupancy of cation sites is retained ($Cu_{5+y}Fe_{1-y}S_4$) exhibit a progressive increase in thermal conductivity with increasing Cu(II) content, principally due to an increased charge-carrier contribution. This contrasts with the behaviour of vacancy-containing phases which exhibit only a weak dependence on hole concentration up to a Cu(II) content of *ca.* 0.15. The combination of an almost compositionally-invariant thermal conductivity and a rising power factor, leads to maximum figures of merit being achieved at Cu(II) contents in the region of 0.10 – 0.15. Moreover, comparison of the two cation-deficient series of materials, $Cu_{5-x}FeS_4$ and $Cu_{4.94+z}Fe_{1-z}S_4$ reveals that in addition to the hole concentration, a critical level of vacancies, in the region of ca. 1%, is required in order to achieve the highest figures of merit as exemplified by $Cu_{4.972}Fe_{0.968}S_4$, which has a Cu(II) content of 0.124 and a vacancy concentration of 1%. This is a nominal vacancy level, based on the ideal formula for bornite, but as shown in Table 1, the compositions determined by EDX are in good agreement with the nominal compositions.

This investigation has led to a significant increase in the maximum ZT of bornite-related phases, as shown in Table 2. A large number of the non-stoichiometric materials reported here exhibit values in the range $0.59 < ZT < 0.80$ at 550K, representing an increase of up to 44%, with respect to previous reports. Although prior to this work, the impact of transition-metal substitution on the TE properties of bornites has been little explored,[29] it has been shown recently that the partial substitution of sulphur by selenium has a significant effect on the transport properties.[34] This suggests that anion substitution, combined with the use of cation substitution coupled with the creation of vacancies described here, may prove to be a highly-effective approach to achieving further enhancements in TE performance.

Table 2. Thermoelectric figures of merit for synthetic bornites

Composition	$(ZT)_{max}$. value	Temperature of $(ZT)_{max}$/K	ZT @ 550K	Reference
$Cu_{4.972}Fe_{0.968}S_4$	0.84	675	0.79	This work
$Cu_5Fe_{1-x}Mn_xS_4$, x=0,0.05,0.1	0.55	540	0.55	29
$Cu_5FeS_{4-x}Se_x$, x=0.4	0.66	675	0.51	34
$Cu_{5+x}Fe_{1-x}S_4$, x=0.04	0.53	700	0.49	23
$Cu_{5.23}Fe_{0.9}S_4$	0.56	680	0.50	35

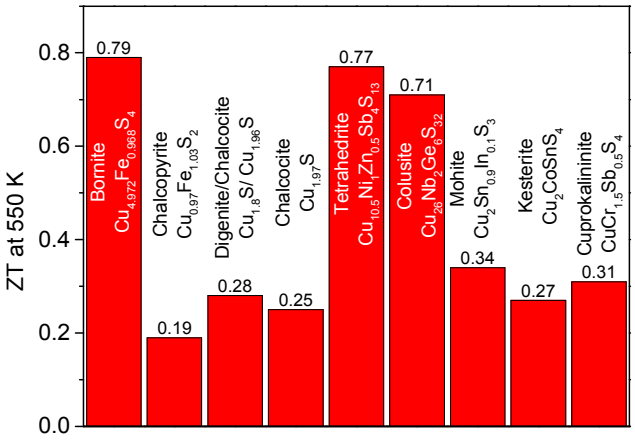

Figure 12. ZT values at 550 K for a range of copper sulphide minerals. The highest reported ZT value for each mineral is given.[15,17,18,43–47]

The high level of interest in copper sulphides for TE applications[15,17,18,43–47] has been driven by a combination of promising performance, coupled with the earth-abundance of the constituent elements.[48] Although materials such as those related to tetrahedrite exhibit a higher absolute maximum figure of merit, the materials reported here are among the highest performing thermoelectrics at temperatures appropriate to energy recovery from low- to mid-range waste heat available in industrial processes (Fig. 12). Indeed the figure of merit of $Cu_{4.972}Fe_{0.968}S_4$ and of substituted tetrahedrites are essentially the same in this temperature range.

Conclusion

The work reported here demonstrates that deviations from the ideal Cu_5FeS_4 stoichiometry produce significant enhancements in the electrical transport properties of bornite, whilst maintaining a low thermal conductivity. This leads to increases of up to 88% in the TE figure of merit. Moreover, the presence of iron on tetrahedral sites appears to suppress the degradation arising from copper ion-mobility in structurally-related PLEC-type materials. Thermal cycling data and constant current stress tests[23] suggest that reasonable device lifetimes could be achievable. Whilst impurity formation, principally chalcopyrite, is evident at higher levels of chemical substitution, this does not significantly impact on the TE properties at low chalcopyrite levels. Bornite-related materials remain relatively unexplored as a class of TE material, suggesting that there is considerable scope to achieve further enhancements in TE performance through chemical substitution.

ASSOCIATED CONTENT

Supporting Information. Powder X-ray diffraction data, DSC data and additional thermal conductivity, electrical property and thermoelectric data. This material is available free of charge via the Internet at http://pubs.acs.org.

AUTHOR INFORMATION

Corresponding Author

*E-mail: a.v.powell@reading.ac.uk

Funding Sources

Financial support from the University Reading and the ISIS neutron facility (STFC) is greatly acknowledged.

ACKNOWLEDGMENT

The authors would like to thank the Science and Technology Facilities Council and The University of Reading for a Facility Development Studentship for S. Long and the Chemical Analysis Facility at The University of Reading for access to X-Ray Diffraction, DSC and SEM equipment.

ABBREVIATIONS

EDX, Energy Dispersive X-Ray; DSC, Differential Scanning Calorimetry; SEM, Scanning Electron Microscope; TE, Thermoelectric, T1, low to intermediate phase transition; T2, intermediate to high phase transition.

REFERENCES

(1) Rowe, D. M. Thermoelectrics, an Environmentally-Friendly Source of Electrical Power. *Renew. Energy* **1999**, *16*, 1251–1256.

(2) Bell, L. E. Cooling, Heating, Generating Power, and Recovering Waste Heat with Thermoelectric Systems. *Science* **2008**, *321*, 1457–1461.

(3) Zhou, Z.; Yang, J.; Jiang, Q.; Li, W.; Luo, Y. Large Improvement of Device Performance by a Synergistic Effect of Photovoltaics and Thermoelectrics. *Nano Energy* **2016**, *22*, 120–128.

(4) Bjørk, R.; Nielsen, K. K. The Performance of a Combined Solar Photovoltaic and Thermoelectric Generator System. *Sol. Energy* **2015**, *120*, 187–194.

(5) Kajikawa, T. Thermoelectric Power Generation System Recovering Industrial Waste Heat. In *Thermoelectrics Handbook: Macro to Nano*; Rowe, D. M., Ed.; CRC Press: Boca Raton, 2006; pp 50-1 - 50–26.

(6) Johnson, I.; Chocate, W. T.; Davidson, A. *Waste Heat Recovery: Technology and Opportunities in U.S. Industry*; United States Department of Energy, Office of Energy Efficiency and Renewable Energy. **2008**, DOI: 10.2172/1218716.

(7) Venkatasubramanian, R.; Siivola, E.; Colpitts, T.; O'Quinn, B. Thin-Film Thermoelectric Devices with High Room-Temperature Figures of Merit. *Nature* **2011**, *413*, 597–602.

(8) Poudel, B.; Hao, Q.; Ma, Y.; Lan, Y.; Minnich, A.; Yu, B.; Yan, X.; Dresselhaus, M. S.; Chen, G.; Ren, Z. High-Thermoelectric Performance of Nanostructured Bismuth Antimony Telluride Bulk Alloys. *Science,* **2008**, 320 (May), 634–638.

(9) Lu, X.; Morelli, D. T. Natural Mineral Tetrahedrite as a Direct Source of Thermoelectric Materials. *Phys. Chem. Chem. Phys.* **2013**, *15*, 5762–5766.

(10) Beeken, R. B.; Garbe, J. J.; Petersen, N. R.; Stoneman, M. R. Electrical Properties of the Ag_6PSe_5X (X=Cl, Br, I) Argyrodites. *J. Phys. Chem. Solids* **2004**, *65*, 1011–1014.

(11) Sun, B.-Z.; Ma, Z.; He, C.; Wu, K. Anisotropic Thermoelectric Properties of Layered compounds in SnX_2(X=S, Se): a promising thermoelectric material. *Phys. Chem. Chem. Phys.* **2015**, *17*, 29844–29853.

(12) Maignan, A.; Guilmeau, E.; Gascoin, F.; Breard, Y.; Hardy, V. Revisiting some chalcogenides for thermoelectricity. *Sci. Technol. Adv. Mater.* **2012**, *13*, 053003.

(13) Ang, R.; Khan, A.U.; Tsujii, N.; Takai, K.; Nakamura, R.; Mori, T. Thermoelectricity Generation and Electron–Magnon Scattering in a Natural Chalcopyrite Mineral from a Deep-Sea Hydrothermal Vent. *Angew. Chem. Int. Ed.* **2015**, *54*, 12909 –12913.

(14) Zhang, R-Z.; Chen, K.; Du, B.; Reece, M.J. Screening for Cu–S based thermoelectric materials using crystal structure features. *J. Mater. Chem. A* **2017**, *5*, 5013–5019.

(15) Khan, A. U.; Al Orabi, R. A. R.; Pakdel, A.; Vaney, J.B.; Fontaine, B.; Gautier, R.; Halet, J.-F.; Mitani, S.; Mori, T. Sb Doping of Metallic $CuCr_2S_4$ as a Route to Highly Improved Thermoelectric Properties. *Chem. Mater.* **2017**, *29*, 2988–2996.

(16) Heo, J.; Laurita, G.; Muir, S.; Subramanian, M. A.; Keszler, D. A. Enhanced Thermoelectric Performance of Synthetic Tetrahedrites. *Chem. Mater.* **2014**, *26*, 2047–2051.

(17) Lu, X.; Morelli, D. T.; Xia, Y.; Ozolins, V. Increasing the Thermoelectric Figure of Merit of Tetrahedrites by Co-Doping with Nickel and Zinc. *Chem. Mater.* **2015**, *27*, 408–413.

(18) He, Y.; Day, T.; Zhang, T.; Liu, H.; Shi, X.; Chen, L.; Snyder, G. J. High Thermoelectric Performance in Non-Toxic Earth-Abundant Copper Sulfide. *Adv. Mater.* **2014**, *26*, 3974–3978.

(19) Liu, H.; Shi, X.; Xu, F.; Zhang, L.; Zhang, W.; Chen, L.; Li, Q.; Uher, C.; Day, T.; Snyder, G. J. Copper Ion Liquid-like Thermoelectrics. *Nat. Mater.* **2012**, *11*, 422–425.

(20) Weldert, K. S.; Zeier, W. G.; Day, T. W.; Panthöfer, M.; Snyder, G. J.; Tremel, W. Thermoelectric Transport in Cu_7PSe_6 with High Copper Ionic Mobility. *J. Am. Chem. Soc.* **2014**, *136*, 12035–12040.

(21) Brown, D. R.; Day, T.; Caillat, T.; Snyder, G. J. Chemical Stability of $(Ag, Cu)_2Se$: A Historical Overview. *J. Electron. Mater.* **2014**, *42*, 2014–2019.

(22) Dennler, G.; Chmielowski, R.; Jacob, S.; Capet, F.; Roussel, P.; Zastrow, S.; Nielsch, K.; Opahle, I.; Madsen, G. K. H. Are Binary Copper Sulfides/ Selenides Really New and Promising Thermoelectric Materials. *Adv. Energy Mater.* **2014**, *4*, 1301581.

(23) Qiu, P.; Zhang, T.; Qiu, Y.; Shi, X.; Chen, L. Sulfide Bornite Thermoelectric Material: A Natural Mineral with Ultralow Thermal Conductivity. *Energy Environ. Sci.* **2014**, *7*, 4000–4006.

(24) Morimoto, N. Structures of Two Polymorphic Forms of Cu_5FeS_4. *Acta Crystallogr.* **1964**, *17*, 351.

(25) Kanazawa, Y.; Koto, K.; Morimoto, N. Bornite: Stability and Crystal Structure of the Intermediate Form. *Canad. Mineral.* **1978**, *16*, 397–404.

(26) Koto, B. Y. K.; Morimoto, N. Superstructure Investigation of Bornite, Cu_5FeS_4, by the Modified Partial Patterson Function. *Acta Crystallogr.* **1975**, *31*, 2268–2273.

(27) Ding, Y. Possible Fe/Cu Ordering Schemes in the 2a Superstructure of Bornite (Cu_5FeS_4). *Amer. Miner.* **2005**, *90*, 1265–1269.

(28) Larson; A.C.; Von Dreele, R.B. General Structure Analysis System. *Los Alamos National Laboratory Report LAUR* **1994**, 86–784.

(29) Guélou, G.; Powell, A. V.; Vaqueiro, P. Ball Milling as an Effective Route for the Preparation of Doped Bornite: Synthesis, Stability and Thermoelectric Properties. *J. Mater. Chem. C* **2015**, *3*, 10624–10629.

(30) Cowan, R. D. Pulse Method of Measuring Thermal Diffusivity at High Temperatures. *J. Appl. Phys.* **1963**, *34*, 926–927.

(31) Ding, Y.; Veblen D.R.; Prewittt, C.T. High-Resolution Transmission Electron Microscopy Study of the 4a and 6a Superstructure of Bornite Cu_5FeS_4. *Amer. Miner.* **2005**, *90*, 1256–1264.

(32) Wiltrout, A. M.; Freymeyer, N. J.; Machani, T.; Rossi, D. P.; Plass, K. E. Phase-Selective Synthesis of Bornite Nanoparticles. *J. Mater. Chem.* **2011**, *21*, 19286.

(33) Grguric, B. A.; Putnis, A. Controls on Phase Transition Temperatures in Bornite: a differential Scanning Calorimetry Study *Canad. Mineral.* **1998**, *36*, 215–226.

(34) Kumar, V. P.; Barbier, T.; Lemoine, P.; Raveau, B.; Nassif, V.; Guilmeau, E. The Crucial Role of Selenium for Sulphur Substitution in the Structural Transitions and Thermoelectric Properties of Cu_5FeS_4 Bornite. *Dalton. Trans.* **2017**, *46*, 2174–2183.

(35) Zhang, A.; Shen, X.; Zhang, Z.; Lu, X.; Yao, W.; Dai, J.; Xie, D.; Guo, L.; Wang, G.; Zhou, X. Large-Scale Colloidal Synthesis of Cu_5FeS_4 Compounds and Their Application in Thermoelectrics. *J. Mater. Chem. C* **2017**, *5*, 301.

(36) Townsend, M. G.; Gosselin, J. R.; Tremblay, R. J.; Ripley, L. G.; Carson, D. W.; Muir, W. B. A Magnetic and Mossbauer Study of Magnetic Ordering and Vacancy Clustering in Cu_5FeS_4. *J. Phys. Chem. Solids* **1977**, *38*, 1153–1159.

(37) Qiu, P.; Shi, X.; Chen, L. Cu-Based Thermoelectric Materials. *Energy Storage Mater.* **2016**, *3*, 85–97.

(38) Olvera, A. A.; Moroz, N. A.; Sahoo, P.; Ren, P.; Bailey, T. P.; Page, A. A.; Uher, C.; Poudeu, P. F. P. Partial Indium Solubility Induces Chemical Stability and Colossal Thermoelectric Figure of Merit in Cu_2Se. *Energy Environ. Sci.* **2017**, *10*, 1668–1676.

(39) Collins, M.F.; Longworth, G.; Townsend, M. G. Magnetic structure of bornite. *Can J. Phys.* **1981**, *59*, 535-539.

(40) van der Laan, G.; Pattrick, R.A.D.; Henderson, C.M.B.; Vaughan, D.J. Oxidation state variations in copper minerals studied with Cu 2p X-ray absorption spectroscopy. *J. Phys. Chem. Solids* **1992**, *53*, 1185-1190.

(41) Di Benedetto, F.; Bernardini, G.P.; Cipriani, C.; Emiliani, C.; Gatteschi, D.; Romanelli, M. The distribution of Cu(II) and the magnetic properties of the synthetic analogue of tetrahedrite: $Cu_{12}Sb_4S_{13}$. *Phys. Chem. Minerals* **2005**, *32*, 155–164

(42) Kumar, V.P.; Paradis-Fortin, L.; Lemoine, P.; Caignaert, V.; Raveau, B.; Malaman, B.; Le Caër, G.; Cordier, S.; Guilmeau, E. Designing a Thermoelectric Copper-Rich Sulfide from a Natural Mineral: Synthetic Germanite $Cu_{22}Fe_8Ge_4S_{32}$ *Inorg. Chem.* **2017**, *56*, 13376-13381.

(43) Ge, Z.-H.; Zhang, B.-P.; Chen, Y.-X.; Yu, Z.-X.; Liu, Y.; Li, J.-F. Synthesis and Transport Property of $Cu_{1.8}S$ as a Promising Thermoelectric Compound. *Chem. Commun.* **2011**, *47*, 12697–12699.

(44) Bouyrie, Y.; Ohta, M.; Suekuni, K.; Kikuchi, Y.; Jood, P.; Yamamotoa, A.; Takabatake, T. Enhancement in the Thermoelectric Performance of colusites $Cu_{26}A_2E_6S_{32}$ (A= Nb, Ta, E= Sn, Ge) using E-site non-stoichiometry. *J. Mater. Chem. C* **2017**, *5*, 4174–4184.

(45) Tan, Q.; Sun, W.; Li, Z.; Li, J. Enhanced Thermoelectric Properties of Earth-Abundant Cu_2SnS_3 via In Doping Effect. *J. Alloys Compd.* **2016**, *672*, 558–563.

(46) Xiao, C.; Li, K.; Zhang, J.; Tong, W.; Liu, Y.; Li, Z.; Huang, P.; Pan, B.; Su, H.; Xie, Y. Magnetic Ions in Wide Band Gap Semiconductor Nanocrystals for Optimized Thermoelectric Properties. *Mater. Horizons* **2014**, *1*, 81–86.

(47) Li, Y.; Zhang, T.; Qin, Y.; Day, T.; Snyder, G. J.; Shi, X.; Chen, L. Thermoelectric Transport Properties of Diamond-like $Cu_{1-x}Fe_{1+x}S_2$ Tetrahedral Compounds. *J. Appl. Phys.* **2014**, *116*, 203705.

(48) Suekuni, K.; Takabatake, T. Research Update : Cu–S Based Synthetic Minerals as Efficient Thermoelectric Materials at Medium Temperatures. *APL Mater.* **2016**, *4*, 104503.

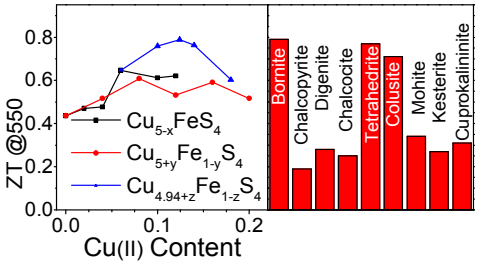
ZT @550
0.0
0.2
0.4
0.6
0.8
0.0
0.1
0.2
Cu(II) Content
$Cu_{5-x}FeS_4$
$Cu_{5+y}Fe_{1-y}S_4$
$Cu_{4.94+z}Fe_{1-z}S_4$
Bornite
Chalcopyrite
Digenite
Chalcocite
Tetrahedrite
Colusite
Mohite
Kesterite
Cuprokalininite